Smart Structures and Systems, Vol. 6, No. 7 (2010) 851-866
DOI: http://dx.doi.org/10.12989/sss.2010.6.7.851

Non-destructive evaluation of concrete quality using PZT transducers

R. Tawie[1], H.K. Lee*[1] and S.H. Park[2]

[1]*Department of Civil and Environmental Engineering, Korea Advanced Institute of Science and Technology, Daejeon 305-701, South Korea*
[2]*Department of Civil and Environmental Engineering, Sungkyunkwan University, Suwon, Gyeonggi 440-746, South Korea*

(Received August 1, 2009, Accepted November 18, 2009)

Abstract. This paper presents a new concept of using PZT (lead zircornate titanate) transducers as a non-destructive testing (NDT) tool for evaluating quality of concrete. Detection of defects in concrete is very important in order to check the integrity of concrete structures. The electro-mechanical impedance (EMI) response of PZT transducers bonded onto a concrete specimen can be used for evaluating local condition of the specimen. Measurements are carried out by electrically exciting the bonded PZT transducers at high frequency range and taking response measurements of the transducers. In this study, the compression test results showed that concrete specimens without sufficient compaction are likely to fall below the desired strength. In addition, the strength of concrete was greatly reduced as the voids in concrete were increased. It was found that the root mean square deviation (RMSD) values yielded between the EMI signatures for concrete specimens in dry and saturated states showed good agreement with the specimens' compressive strength and permeable voids. A quality metric was introduced for predicting the quality of concrete based on the dry-saturated state of concrete specimens. The simplicity of the method and the current development towards low cost and portable impedance measuring system, offer an advantage over other NDE methods for evaluating concrete quality.

Keywords: electro-mechanical impedance; PZT transducers; non-destructive testing; concrete quality.

1. Introduction

In the past decade, the electro-mechanical impedance (EMI) sensing method has received considerable interest among researchers. This method is based on unique properties of piezoelectric materials. Piezoelectric materials are most widely used as sensors and/or actuators. As an actuator, a piezoelectric material when applied with an electric field produces mechanical strains proportional to the electrical field, and conversely, as a sensor, it gives off electrical discharge (voltage) when it is deformed. PZT (lead-zirconate-titanate) and macrofiber composites (MFC) patches are the two most common commercialized products used as sensors/actuators in the field of structural health monitoring (SHM) and non-destructive evaluation (NDE) (Park *et al*. 2009b).

Compared to other NDE methods such as Schmidt hammer, impact-echo, ultrasonic pulse velocity, acoustic emission, ground penetrating radar, infrared thermography and microwaves, the EMI

*Corresponding author, E-mail: leeh@kaist.ac.kr

method has been demonstrated for wider applications (Park *et al*. 2003). For example, Sun *et al*. (1995), who was first to apply the method, investigated the integrity of truss structures and introduced a scalar damage metric known as the root mean square deviation (RMSD). Chaudhry *et al*. (1995, 1996) demonstrated the effectiveness of the PZT transducers for detecting localized alteration due to bolt loosening and for monitoring crack and bonding of composite patched repairs. Tseng *et al*. (2002) investigated capability of surfaced bonded PZT transducers to detect void and crack in concrete by numerical simulation. Dugnani and Chang (2002) developed a novel approach using the EMI method for characterizing unstable atherosclerotic plaque. Other works using the EMI method for monitoring of civil structures can be found in Kim *et al*. (2009), Sohn *et al*. (2008) and Park *et al*. (2005).

The EMI method has also shown great potential for monitoring corrosion (Simmers Jr. 2005, Park *et al*. 2007) and strength development of concrete (Soh and Bhalla 2005, Shin *et al*. 2008, Tawie and Lee 2010). Based on the EMI principle, Park *et al*. (2007) used an active sensing device consisting of an impedance measuring chip (AD5933) and a MFC patch to detect and quantify corrosion in an aluminum sample. In monitoring hardening of concrete during curing process, Soh and Bhalla (2005) found a strong correlation between cube compressive strength of concrete and resonant frequency of the EMI signature. Shin *et al*. (2008) investigated the effect of different curing methods on the EMI resonance signatures, while several statistics metrics were compared to evaluate the resonance frequency shift of PZT patches bonded onto concrete cubes of different mix proportions and empirical function was proposed to predict the relative strength gain of concrete in an earlier work by the authors (Tawie and Lee 2010).

Maintenance and repairs of concrete structures are major issues throughout the world today due to huge amount of money spent each year. In Europe, some 50% of the annual construction budget is spent on remediation and retrofitting of existing buildings and infrastructures (Matthews and Morlidge 2008). Premature deterioration of concrete structures may occur due to poor quality of concrete. The quality of concrete depends on quality of materials supplied to the site, construction techniques, workmanship and exposures (Bungey and Millard 1996). Many researches have shown that deterioration of concrete is linked to its pore structure since permeability, which is a primary factor in determining durability of concrete, is closely related to porosity or volume of pores in concrete (Mehta and Monteiro 2006). Detwiler (1996) summarized that permeability of concrete is the cause of most of damage mechanisms such as carbonation and chloride attack. Patel *et al*. (1995) reported that curing temperature and relative humidity influence the strength development, microstructure and long term durability of concrete. Bork and Preben (1989) explained that presence of entrapped air voids could be an indication of inadequate compaction.

This research was motivated by the numerical findings by Tseng *et al*. (2002). The EMI method was shown to be applicable for detecting void in concrete and good correlation was observed between the RMSD index, used for evaluating the damage, and void size and depth. The authors (Tawie *et al*. 2009) had also conducted an initial experimental investigation on two 100 (diameter) × 50 (height) mm cylindrical specimens to investigate whether the EMI response of PZT transducers bonded onto concrete surface can be qualitatively used to show the difference between a specimen without defect versus a specimen with simulated defects (drilled holes). As shown by the authors in Tawie *et al*. (2009), the difference was quite clear and this indicated that the EMI response of the PZT transducers was influenced by the change in the physical properties of concrete. In the present study, we conducted further EMI measurements on concrete specimens with varying compaction quality and under dry and saturated states.

2. Theoretical background

The basic of the EMI sensing method is that information about a structure can be obtained by electrically exciting the PZT transducers bonded on the structure at high frequencies in the range of 30 to 400 kHz using alternating electrical field source and taking response measurements of the transducers (Park *et al*. 2003). PZT transducers can capture dynamic response in the structure in the form of coupled electro-mechanical admittance that serves as a function of the interaction between the electrical and mechanical properties of the sensors and the structure, respectively (Liang *et al*. 1996). Liang *et al*. (1996) derived the electro-mechanical admittance, as measured at the terminals of a PZT transducer attached to a host structure, as follows

$$Y = j\omega\frac{wl}{h}\left[\bar{\varepsilon}_{33}^{T} - \frac{Z_S}{Z_S + Z_A}d_{31}^2\bar{Y}_{11}^{E}\right] \tag{1}$$

where j is $\sqrt{-1}$, ω is the angular frequency, w, l and h are the width, length and thickness of the PZT transducer, respectively, $\bar{\varepsilon}_{33}^{T}$ is the complex electric permittivity of the transducer (at constant stress field), Z_S is the structural impedance, Z_A is the transducer impedance, d_{31} is a piezoelectric strain coefficient and $\bar{Y}_{11}^{E}$ is the complex Young's modulus of the transducer (at constant electric field). The resonance of the electro-mechanical PZT transducer-structure system occurs when the Z_A and Z_S match (Liang *et al*. 1996).

Note that electrical impedance Z is a complex number, made up of real and imaginary parts as follows (Agilent 2009)

$$Z = R + jX \tag{2}$$

where R is the resistance (measured in ohms) and X is the reactance (measured in ohms). Admittance is the inverse of impedance. Thus (Agilent 2009)

$$Y = Z^{-1} = \frac{1}{R + jX} = \left(\frac{R}{R^2 + X^2}\right) + j\left(\frac{-X}{R^2 + X^2}\right) \tag{3}$$

Just like impedance, admittance is composed of real and imaginary parts as follows (Agilent 2009)

$$Y = G + jB \tag{4}$$

where G is the conductance and B is the susceptance, both measured in siemens. G and B are given by Eqs. (5) and (6), respectively, as follows (Agilent 2009)

$$G = \Re(Y) = \left(\frac{R}{R^2 + X^2}\right) \tag{5}$$

$$B = \Im(Y) = \left(\frac{-X}{R^2 + X^2}\right) \tag{6}$$

The magnitude and phase of the admittance are given by Eqs. (7) and (8), respectively, as follows (Agilent 2009)

$$|Y| = \sqrt{G^2 + B^2} = \frac{1}{\sqrt{R^2 + X^2}} \tag{7}$$

$$\angle Y = \tan^{-1}\left(\frac{B}{G}\right) = \tan^{-1}\left(\frac{-X}{R}\right) \tag{8}$$

In general, only the real parts are used for SHM or NDE, while the imaginary parts are not considered since the dielectric constant $\bar{\varepsilon}_{33}^{T}$, which is temperature sensitive, only affects the imaginary parts (Park *et al*. 2003). Recently, Bhalla *et al*. (2009) demonstrated that the real parts G of the measured admittance are more sensitive to damage than other parameters considered in their study that includes B, $|Y|$, $|Z|$, B_A and $|Y_A|$. B_A and $|Y_A|$ are active components of B and $|Y|$, respectively. Details of the decomposition of the active B_A and $|Y_A|$ can be found in Bhalla and Soh (2003). Meanwhile, Kim *et al*. (2007) employed B in addition to G for damage identification while Park *et al*. (2006, 2009a) showed that B can be used to diagnose the integrity of the bonded PZT transducers.

3. Experimental program

3.1 Specimen preparation

Since the objective of this study was to investigate the efficacy of the EMI method for evaluating quality of concrete specimens, several cylindrical specimens with varying compaction quality were prepared as shown in Fig. 1. All the specimens were made with the same concrete mix proportion as shown in Table 1. The properties of the constituent materials are given in Table 2. The mix proportion was designed based on the absolute volumes of the constituent materials as per ACI Committee 211 (2001). The batch weights of the constituent materials were calculated from the total volume of specimens to be prepared plus 15% extra to take into account the loss during mixing and molding of test specimens.

The constituent materials were mixed in a pan mixer and the mixtures were cast in standard size cylindrical molds (100 × 200 mm). The first three types of the specimens were compacted by rodding with a tamping rod. The compaction quality by rodding is classified as poor (type 1), moderate (type 2) and good (type 3) based on the number of roddings: 8, 16 and 25 per layer, respectively. The last type of specimen was compacted by internal vibration (one insertion per layer) and classified as type 4. All specimens were compacted in the molds with two layers of approximate equal depth in accordance to

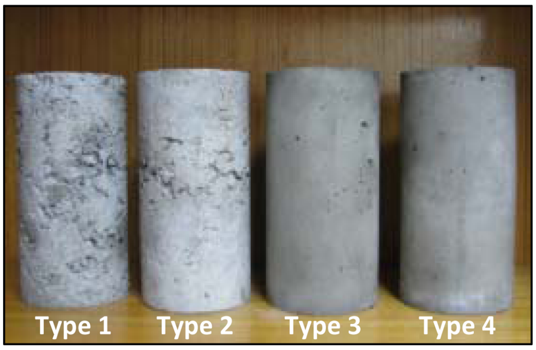

Fig. 1 Concrete specimens with varying compaction quality

Table 1 Concrete mix proportion

Cement (kg/m^3)	Water (kg/m^3)	Fine aggregate (kg/m^3)	Coarse aggregate (kg/m^3)
442	199	775	858

Table 2 Properties of materials

Material	Property
Portland cement	Specific gravity: 3.15
River sand (Fine aggregate)	Fineness modulus: 2.51 Specific gravity: 2.56 Absorption: 1.73%
Crushed gravel (Coarse aggregate)	Dry rodded unit weight: 1480 kg/m^3 Specific gravity: 2.58 Absorption: 0.34% Maximum size: 12.5 mm
Tap water	Density: 998~1000 kg/m^3

the ASTM C192 (2002). Immediately after casting, the specimens were covered with plastic sheets to prevent moisture loss and stored in a curing room at 20 °C for 24 hours before the specimens were removed from the molds. All specimens were marked and put in a water tank in the curing room until 28 days of age. In total, sixteen 100 × 200 mm cylindrical specimens were prepared: twelve used for compression tests and four for both porosity and EMI measurements. The porosity tests and EMI measurements were performed on 100 × 50 mm cylinders which were cut from the 100 × 200 mm cylinders.

3.2 Characterization tests

3.2.1 Compression test

Compressive strength is one of the most important parameters used for quality control of concrete. Three specimens were used to determine the compressive strength of each specimen type at 28 days of curing in accordance to the ASTM C39 (2002). Compression tests were carried out using a universal testing machine (UTM). The UTM was operated under the displacement control at a constant head-loading rate of 0.015 mm/sec.

3.2.2 Porosity test

Porosity tests for determining the permeable voids in concrete specimens were conducted according to the ASTM C642 (2002). At 28 days, the submerged specimens in the water tank were taken out and surface-dried with a towel to determine the saturated surface-dry mass of the specimens in air, W_s. The specimens were then soaked in the water to determine their buoyant mass, W_b. After that the specimens were put in the oven at 105 ºC for more than 48 hours and then allowed to cool to a final temperature of 20 to 25 ºC before the oven-dry mass, W_d was determined. The permeable voids of concrete were calculated from the ratio of weight increase due to water absorption and weight decrease because of buoyancy. The following equation from the ASTM C642 (2002) was used to calculate the permeable voids of concrete

$$\text{Permeable voids (\%)} = \frac{W_s - W_d}{W_s - W_b} \times 100 \tag{9}$$

3.3 EMI measurement

The EMI measurement set-up consists of a concrete specimen to be tested, a PZT transducer bonded

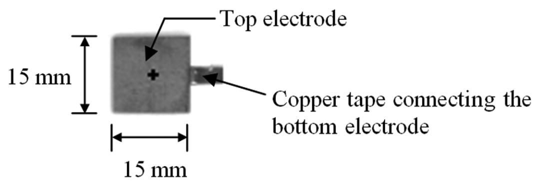

Fig. 2 PZT transducer (15 × 15 × 0.508 mm)

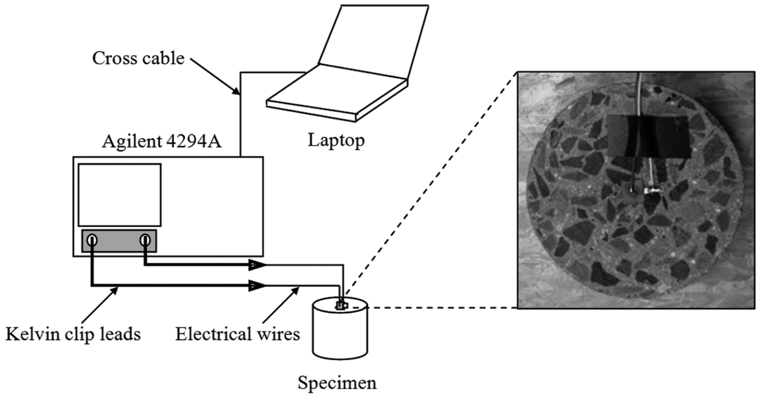

Fig. 3 Experimental setup for EMI sensing method

onto the concrete surface, an impedance analyzer, a Kelvin clip leads and electrical wire connections. A PZT transducer of size 15-by-15 square mm and 0.508 mm thickness cutout from a single PSI-5A4E sheet (Piezo System 2009) is shown in Fig. 2. Fig. 3 shows the schematic diagram of the measurement set-up. In this study, the PZT transducers were bonded using epoxy adhesive (Loctite 2009) consisting of two parts - resin and hardener mixed together. The adhesive is water resistant and cures rapidly at room temperature. In order to bond a PZT transducer with uniform thickness of adhesive layer, a thin plastic sheet with a square hole (16 × 16 mm) was laid on the concrete surface before spreading the adhesive uniformly inside the hole using the thickness of the plastic sheet as a control. After wiping off excess adhesive with a cloth, the PZT transducer was attached and light pressure was applied over the top surface of the PZT for several minutes. Finally, the plastic sheet was removed and the PZT was left undisturbed for at least 24 hours at room temperature to facilitate complete curing of the adhesive.

To conduct the EMI measurements, the impedance analyzer was set to measure G (real parts of admittance) from 0.04 kHz to 250 kHz using the trigger function by a single sweep. Bandwidth of 4 was selected (5 the most precise) and the measured EMI signatures consisted of a total of 801 data points. Measurements were taken several times to observe the repeatability and after each measurement the data was saved in the memory of the impedance analyzer. The data was later transferred from the impedance analyzer to a laptop computer by a simple data acquisition technique using a cross cable as shown in Fig. 3.

In this study, EMI measurements were conducted for each specimen type under the dry and saturated states. The fully dried state was achieved by oven-drying the specimens for 48 hours at 105 ^{o}C and the specimens were allowed to cool to the room temperature before measurements were taken. In order to perform measurements on specimens in saturated state, the specimens were soaked under water slightly below the top surface in a container. To protect the PZT transducers against accidental overflow of water, the transducers were sealed with water-proofing silicon grease (Dow Corning 2009). To achieve the saturation stage, the specimens were weighed every 24 hours to check the increase in mass until the increase was less than 0.5% of the larger value. The specimens were found to reach the saturation stage within 72 hours after soaking. The saturated specimens were wrapped with air bubble plastic to prevent moisture loss and the EMI measurements were conducted immediately.

4. Measurement reliability

Previous researches have shown that the EMI response of PZT is affected by the environmental conditions. Temperature changes could lead to changes in electrical and mechanical properties of all the components, including PZT patches, adhesive layer and host structure (Yang *et al*. 2008). In this study, the EMI measurements for each specimen type (dry and saturated condition) were conducted at a room temperature of 24±0.3 °C. Since the variation in the temperature was negligible, the temperature effect to the EMI response of the bonded PZT transducers is considered minimal. Otherwise, a temperature compensation technique (e.g., Koo *et al*. 2007) can be employed.

A critical issue in the application of the EMI sensing method is that the PZT transducers need to be diagnosed before each measurement is taken. This is because damage in the transducers may significantly affect their performance and lead to false results. In order to assess the condition of the PZT transducers, a technique developed by Park *et al*. (2006, 2009a) was employed in this study. The diagnostic technique is capable of evaluating the integrity of the bonded PZT transducers. Park *et al*. (2006, 2009a) showed that a change in the slope of the imaginary part B of the admittance can be used to indicate damage in PZT transducers or poor bonding of the transducers.

5. Results and discussion

5.1 Compression and porosity test results

The average compressive strength of each specimen type is given in Table 3. The values shown in the bracket are the relative average strength of the specimens normalized to the design strength of 37 MPa as per ACI Committee 211 (2001). Fig. 4 presents the results of the porosity test. A regression between the two parameters as shown in Fig. 5 indicates that compressive strength is inversely proportional to the permeable voids. In general, the compressive strength and permeable voids of concrete in early curing stage are much lower and greater, respectively, than at 28 days of curing (Safiuddin and Hearn 2005). Although oven drying at 100 to 110 °C is a standard ASTM procedure for determining the dried weight of concrete specimens, the drying procedure is still a controversial issue among researchers.

Table 3 Compressive strength of specimens

Specimen type	Compaction method	Compressive strength (MPa)
1	Rodding - 8 times	22.26 (0.61)
2	Rodding - 16 times	35.14 (0.95)
3	Rodding - 25 times	39.80 (1.08)
4	Vibration - 10 s	40.31 (1.09)

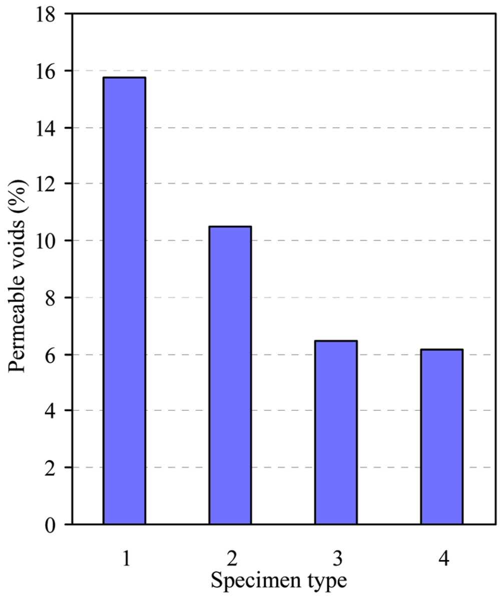

Fig. 4 Permeable voids of specimens

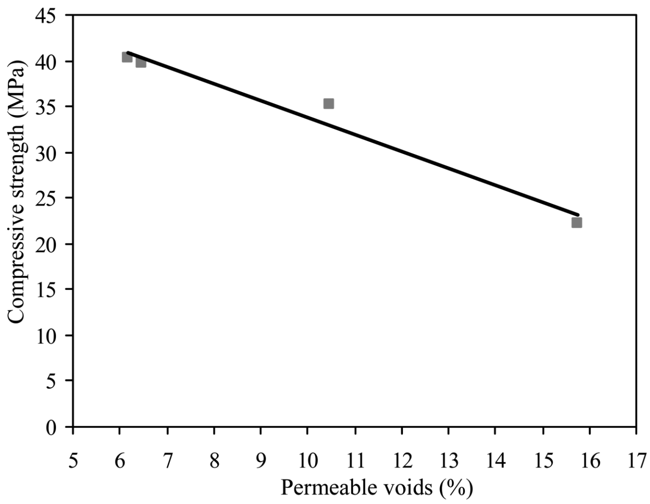

Fig. 5 Compressive strength versus permeable voids

According to Bahador and Cahyadi (2009), a few days of 105 ºC oven drying may increase the pore size diameter by up to four times in addition to significantly increase the pore connection. However, this issue is beyond the scope of this study and it should be the subject of future research.

It is as expected that the compaction quality significantly influenced the compressive strength and permeable voids (porosity) of concrete. The strength of the specimen types 1 and 2 was 40% and 5% lower than the design strength, while that of types 3 and 4 was close to 10% higher than the design strength. The permeable voids increased approximately by 4% and 9%, respectively, when the number of compaction by rodding was reduced from 25 times to 16 and 8 times. There is no much difference in compressive strength and permeable voids between specimen types 3 and 4. This indicates that maximum potential strength in concrete can be accomplished with sufficient compaction. It is noted that it will be easier to achieve full compaction by vibration for low-workable concrete and a properly vibrated concrete will have good finishes and optimal strength and durability. While under vibration may cause honeycombing, over vibration may cause segregation of coarse aggregates (Mehta and Monteiro 2006).

5.2 EMI measurement results

5.2.1 General

Figs. 6(a)-(d) present the average real parts (*G*) of admittance as measured by the bonded PZT transducers from three measurements for each of the specimen type, respectively. The admittance signature for an unbonded PZT transducer is also shown for comparison. It is shown that the act of bonding a PZT transducer on concrete surface caused the signature to shift to the right and the peak magnitude dropped significantly. The adhesive layer provided the medium for the interaction between the PZT and the concrete specimens. The electro-mechanical coupling represented by the Eq. (1) is the basis for the application of the EMI sensing method in this research and experimentally we can obtain the parameter such as *G* to investigate the state of concrete by qualitatively comparing the EMI signatures of the bonded PZT transducers.

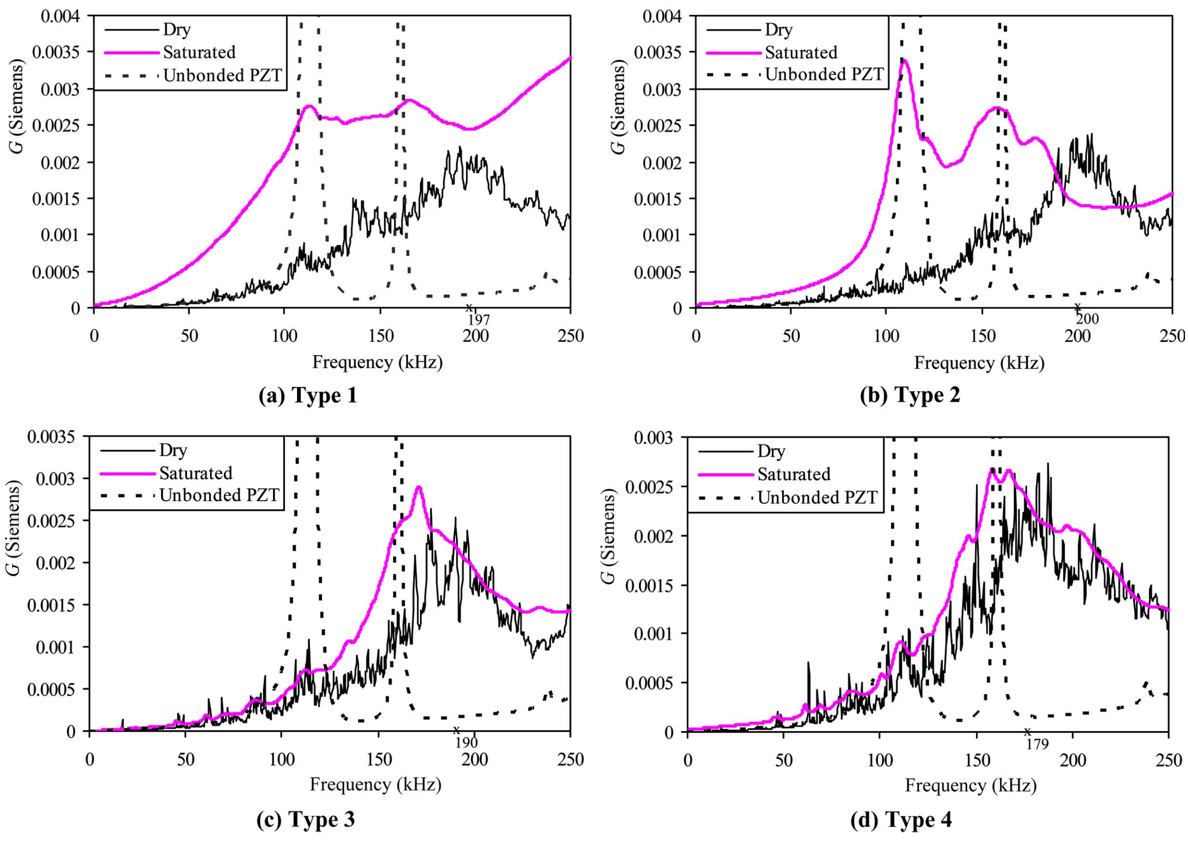

Fig. 6 Real parts (*G*) of the measured admittance for all the specimen types

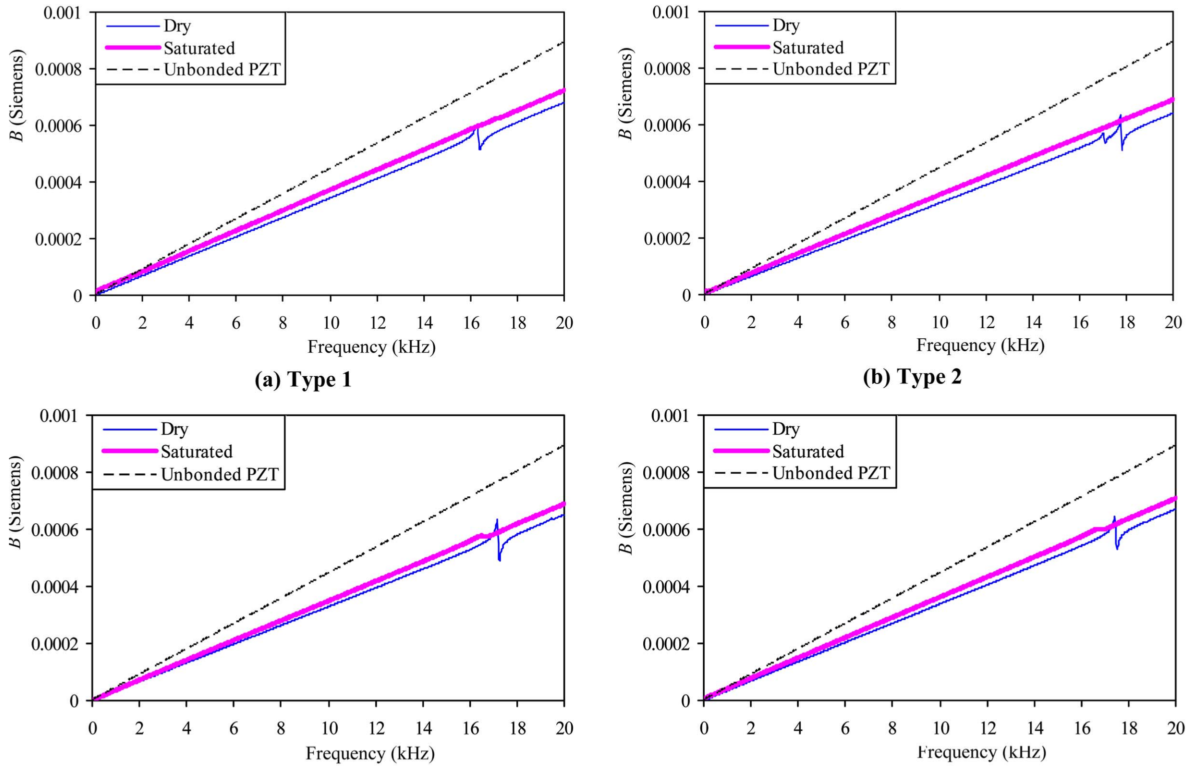

(a) Type 1 (b) Type 2

(c) Type 3 (d) Type 4

Fig. 7 Imaginary parts (B) of the measured admittance for all the specimen types

5.2.2 Diagnostic test results

Prior to the EMI measurements on the specimens, the diagnostic tests were conducted by measuring the imaginary parts (B) of the PZT admittance from 0.04 kHz to 20 kHz. Results of the PZT diagnostic tests are shown in Figs. 7(a)-(d). According to Park *et al.* (2009a), it is desirable for the bonded PZT transducers to exhibit responses with the same slope and for that slope to be lower than that of an unbonded PZT. In the figures, the slope of the measured B values of the unbonded PZT is used as an indicator to identify total de-bonding of the PZT transducers from the concrete surface. It can be seen that the slopes of the B values of that bonded PZT transducers for both the dry and saturated states are much lower than that of an unbonded PZT. The diagnostic test results confirm that all PZT transducers were installed properly and no damage occurred in the transducers.

5.2.3 EMI signatures for the dry state

At first, it was expected that the dry state signatures could reveal the qualitative difference in the four specimens made with varying compaction quality. While theoretically, we should be able to observe the difference in the EMI signatures between a poor and a good quality concrete specimens, the results obtained from the experiments did not yield a clear difference between the two signatures. As we can see in Figs. 6(a)-(d), there is not enough evidence in terms of resonance frequency shifts or peaks that can be observed for the poor (type 1) and moderate (type 2) quality specimens. This could primarily indicate that there are variations in the performance of the PZT transducers or non-uniformity in bonding strength and condition (Tseng and Naidu 2002). From the figures, we can take note of the resonance frequencies of the dry state signatures. The true resonance frequencies for the dry state signatures are difficult to identify due to existence of many peaks in the resonance region and therefore estimated around the centre of the resonance regions. Roughly, the centre resonance (marked 'x') of the EMI signatures of the bonded PZT transducers for the dry state is located at 197, 200, 190 and 176 kHz, respectively, for specimen types 1, 2, 3 and 4. For comparison, the first resonance frequency for the unbonded PZT transducer is 114 kHz.

5.2.4 EMI signatures for the saturated state

Interestingly, we can clearly observe the qualitative difference in the EMI signatures for the saturated state as shown in Figs. 6(a)-(d). Compared to the signatures for the good quality specimens (types 3 and 4), it can be seen from Figs. 6(a) and (b) that the corresponding changes in the signatures from dry to saturated state are greater for specimen types 1 and 2 that represent concrete quality of poor and moderate compaction, respectively. From the figures, we can observe that the resonance frequencies shifted to the left due to the water absorption within the concrete. On account of the resonance frequency shifts from dry to saturated state, the amount of frequency shift for specimen types 1, 2, 3 and 4 was 85, 89, 18 and 17 kHz. Looking at these values, specimen types 1 and 2 have approximately the same frequency shift, and the same in the case of types 3 and 4 with much lower amount. As we have seen in Fig. 4, the amount of permeable voids in specimen types 1 and 2 are approximately twice that of types 3 and 4. According to Rossi (1991), the concrete mechanical properties change with amount and distribution of voids and presence of water within the permeable pore structure. The explanation is consistent with the observation of Yaman *et al*. (2002), and this could be the reason for the change in the EMI signatures of the bonded PZT transducers from dry to saturated state.

The EMI measurement results showed that water absorption in concrete can affect the EMI signatures. So far, none of the researchers who applied the EMI method for damage detection in concrete structures have investigated the effect of water absorption in concrete. Most of these studies were conducted in a controlled laboratory condition where the structures are not exposed to the environments. The significance of the findings in the present study is that in the implementation of the EMI method for SHM of concrete structures such as bridges, the change in moisture state in concrete could create false alarms if the effect is not taken into account.

5.3 Data processing of EMI signatures

In the present EMI method, the indicator of defects or damages in structures is based the deviation in the baseline signature. The baseline signature is normally taken for the pristine or healthy case of structures and to be compared with the damage case. For processing the difference between the baseline and the damaged signatures, a statistics metric such as the root mean square deviation (RMSD) metric can be used (Giurgiutiu 2008). In this study, we applied the baseline approach based on the dry-saturated state of the concrete specimens. The RMSD metric given in Eq. (10) is used to compare the EMI signatures for the dry and saturated states point by point, and the difference is squared, summed and then normalized by the sum of the square of the G values for the dry state. By taking the square root of the calculation, we obtain the RMSD value (Giurgiutiu 2008).

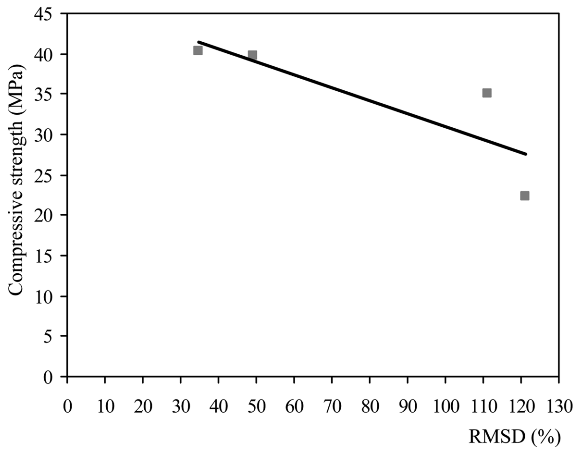

Fig. 8 RMSD values versus compressive strength

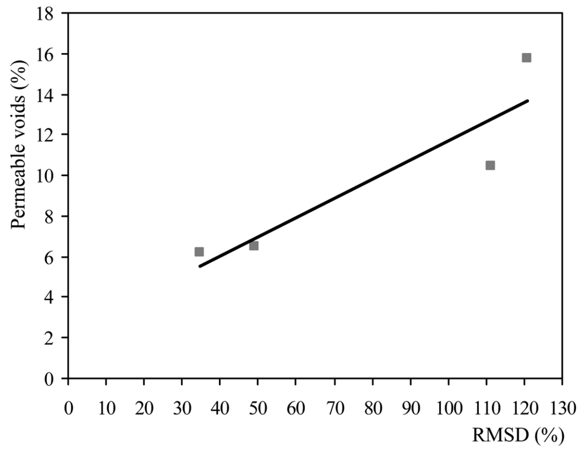

Fig. 9 RMSD values versus permeable voids

$$\text{RMSD (\%)} = \sqrt{\frac{\sum_N [G_i^o - G_i^x]^2}{\sum_N [G_i^x]^2}} \times 100 \tag{10}$$

The calculated RMSD values were compared with the corresponding compressive strength and permeable voids for each of the specimen type in Figs. 8 and 9, respectively. From the figures, we can see that as the RMSD value increases, compressive strength and permeable voids decreases and increases, respectively. Using a linear regression model, the relationship between the RMSD values and the compressive strength (σ_c) and permeable voids (P), respectively, are given by the following Eqs. (11) and (12)

$$\sigma_c = -0.1604(\text{RMSD}) + 47.048 \tag{11}$$

$$P = 0.0938(\text{RMSD}) + 2.312 \tag{12}$$

where the RMSD value is given in percent. The correlation coefficients (r) for the Eqs. (11) and (12) are 0.8296 and 0.9109, respectively. Based on these r values, it can be said that the RMSD values show good correlation with the concrete specimens' compressive strength and permeable voids.

In order to evaluate defects more meaningfully, the RMSD metric values are normalized by a reference metric value as follows (Ayres *et al*. 1998, Rickli and Camelio 2009)

$$D = \frac{\text{RMSD}}{\text{RMSD}_{\text{REF}}} \times 100 \tag{13}$$

where D is the new metric, RMSD is the original metric and RMSD_{REF} is the metric for a concrete specimen with good quality i.e., acceptable strength and porosity. The application of this new metric for evaluating quality of concrete specimens in this study is shown in Fig. 10 where the specimen type 3 was chosen as the reference specimen. In Fig. 10, values that are less than 100% signify that the particular

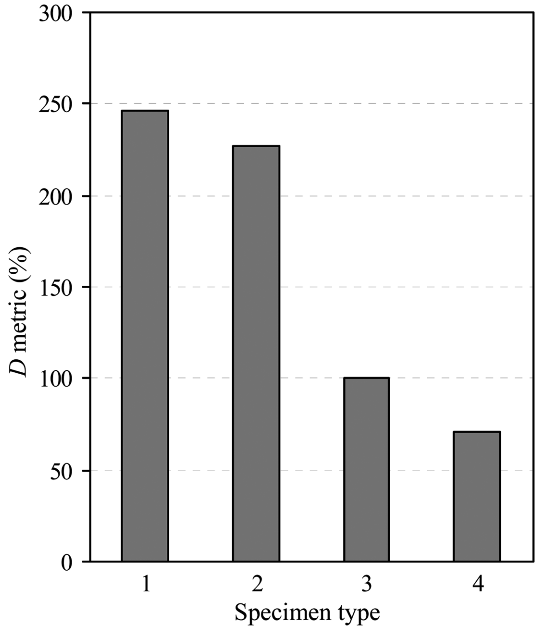

Fig. 10 Characterization of quality of specimens

concrete specimens have better quality than the reference specimen, while values exceeding 100% signify the particular specimens are of unacceptable quality and should be rejected. Note that a value above 100% in Eq. (13) does not guarantee that a sample has more porosity and lower strength due to variability in the measurement system and concrete specimens.

6. Conclusions

This paper presents the effort to extend the applicability of the EMI sensing method using PZT transducers as a non-destructive testing (NDT) tool for evaluating quality of concrete specimens. Real parts of the electrical admittance of PZT transducers bonded on concrete specimens with varying compaction quality were measured using an impedance analyzer at frequency ranging from 0.04 kHz to 250 kHz. In addition, compression and porosity tests were conducted to characterize the properties of the prepared specimens. The reliability of the EMI measurements, which depends on the integrity of the bonded PZT transducers, was verified by performing the diagnostic tests using imaginary parts of the measured electrical admittance of the bonded PZT transducers.

It was shown that concrete specimens without sufficient compaction are likely to fall below the desired strength, and the strength of concrete was greatly reduced as the voids in concrete were increased. As water was absorbed within the permeable pore structure of concrete, the EMI measurement results showed that the EMI signatures also changed with the change in moisture state in the concrete specimens. The EMI response of the bonded PZT transducers on the concrete specimens for the saturated state was found to be correlating well with the compaction quality of the specimens. The change in the EMI signatures of the bonded PZT transducers from dry to saturated state was quantified using the RMSD metric, and it was found that the RMSD metric values showed good agreement with the concrete specimens' compressive strength and permeable voids. Based on the RMSD metric values, a quality metric was introduced for predicting the quality of concrete.

A study would be carried out based on the current work, focusing on theoretical basis for the frequencies to obtain a clearer understanding of the changes in the EMI signatures due to concrete age, moisture content and other factors. In spite of the diagnosis tests conducted to ensure reliability of the EMI results, future tests would also address the reproducibility of the results using at least two PZTs attached to the same specimen and more specimens would be tested for obtaining a better correlation between RMSD values and compressive strength and permeable voids of concrete. Effect of drying temperature and methods, PZT attachment techniques, PZT type and size would also be investigated.

Acknowledgements

This research was financially supported by the Korea Science and Engineering Foundation (KOSEF) through a grant provided by the Korean government (MEST: 20090080587).

References

ACI Committee 211 (2001), *Standard practice for selecting proportions for normal, heavyweight, and mass concrete*, ACI Manual of Concrete Practice, Part 1, American Concrete Institute, Michigan, USA.

Agilent (2009), *Agilent Impedance Measurement Handbook: A guide to measurement technology and techniques*, 4th Edition, http://cp.literature.agilent.com/litweb/pdf/5950-3000.pdf.

ASTM C192 (2002), *Standard practice for making and curing concrete test specimens in the laboratory*, Annual Book of ASTM Standards, American Society for Testing and Materials, Philadelphia.

ASTM C39 (2002), *Standard test method for compressive strength of cylindrical concrete specimens*, Annual Book of ASTM Standards, American Society for Testing and Materials, Philadelphia.

ASTM C642 (2002), *Standard test method for density, absorption and voids in hardened concrete*, Annual Book of ASTM Standards, American Society for Testing and Materials, Philadelphia.

Ayres, J.W., Lalande, F., Chaudhry, Z.A. and Rogers, C.A. (1998), "Qualitative impedance based health monitoring of civil infrastructures", *Smart Mater. Struct.*, **7**(5), 599-605.

Bahador, S.D. and Cahyadi, J.H. (2009), "Modeling of carbonation of PC and blended cement concrete", *IES J. Part A: Civ. Struct. Eng.*, **2**(1), 59-67.

Bhalla, S. and Soh, C.K. (2003), "Structural impedance based damage diagnosis by piezo-transducers", *Earthq. Eng. Struct. D.*, **32**(12), 1897-1916.

Bhalla, S., Gupta, A., Bansal, S. and Garg, T. (2009), "Ultra low-cost adaptations of electro-mechanical impedance technique for structural health monitoring", *J. Intel. Mat. Syst. Str.*, **20**(8), 991-999.

Bork, J.B. and Preben, C. (1989), "Petrograhic examination of hardened concrete", *Bull. Eng. Geol. Environ.*, **39**(1), 99-103.

Bungey, J.H. and Millard, S.G. (1996), *Testing of Concrete in Structures*, 3rd Edition, Blackie Academic & Professional, London, UK.

Chaudhry, Z.A., Joseph T., Sun, F.P. and Rogers, C.A. (1995), "Local-area health monitoring of aircraft via piezoelectric actuator/sensor patches", *Proceedings of the SPIE North American Conference on Smart Structures and Materials*, San Diego, CA, USA, March.

Chaudhry, Z.A., Lalande, F., Ganino, A. and Rogers, C.A. (1996), *Monitoring the integrity of composite patch structural repair via piezoelectric actuators/sensors*, AIAA-1996-1074-CP.

Detwiler, R.J. (1996), *Microstructure and mass transport in concrete, Integrated Design and Environmental Issues in Concrete Technology* (Ed. K. Sakai), E & FN Spon, London, UK.

Dow Corning (2009), *Data sheet,* http://www.dowcorning.com.

Dugnani, R. and Chang, F.K. (2002), “A novel impedance-based sensor technique for real time, in vivo, unstable plaque characterization”, *Proceedings of the 1st European Workshop on Structural Health Monitoring*, Paris, France, July.

Giurgiutiu, V. (2008), *Structural health monitoring with piezoelectric wafer active sensors*, Elsevier, London, UK.

Kim, J., Grisso, B.L., Ha, D.S. and Inman, D.J. (2007), “An all-digital low-power structural health monitoring system”, *Proceedings of the IEEE Conference on Technologies for Homeland Security*, Woburn, MA, USA, May.

Kim, J.T., Park, J.H., Hong, D.S., Cho, H.M., Na, W.B. and Yi, J.H. (2009), “Vibration and impedance monitoring for prestress-loss prediction in PSC girder bridges”, *Smart Struct. Syst*., **5**(1), 81-94.

Koo, K.Y., Park, S., Lee, J.J., Yun, C.B. and Inman, D.J. (2007), “Impedance-based structural health monitoring considering temperature effects”, *Proceedings of the Health monitoring of structural and biological systems*, San Diego, CA, USA, March.

Liang, C., Sun, F. and Rogers, C.A. (1996), “Electro-mechanical impedance modeling of active material systems”, *Smart Mater. Struct*., **5**, 171-186.

Loctite (2009), *Product catalog,* http://www.loctiteproducts.com.

Matthews, S. and Morlidge, J. (2008), “Achieving durable repaired concrete structures - a performance-based approach”, *P. I. Civil Eng.-Str. B*., **161**(1), 17-28.

Mehta, P.K. and Monteiro, P.J.M. (2006), *Concrete: microstructure, properties, and materials*, 3rd Edition, Mc Graw Hill, New York, USA.

Park, G., Farrar, C.R., Rutherford, C.A. and Robertson, A.N. (2006), “Piezoelectric active sensor self-diagnosis using electrical admittance measurements”, *J. Vib. Acoust*., **128**(4), 469-476.

Park, G., Sohn, H., Farrar, C.R. and Inman, D.J. (2003), “Overview of piezoelectric impedance-based health monitoring and path forward”, *Shock Vib. Digest*, **35**(6), 451-463.

Park, S., Grisso, B.L., Inman, D.J. and Yun, C.B. (2007), “MFC-based structural health monitoring using a miniaturized impedance measuring chip for corrosion detection”, *Res. Nondestruct. Eval*., **18**(2), 139-150.

Park, S., Park, G., Yun, C.B. and Farrar, C.R. (2009a), “Sensor self-diagnosis using a modified impedance model for active sensing-based structural health monitoring”, *Struct. Health Monit*., **8**(1), 71-82.

Park, S., Shin, H.H. and Yun, C.B. (2009b), “Wireless impedance sensor nodes for functions of structural damage identification and sensor self-diagnosis”, *Smart Mater. Struct*., **18**(5).

Park, S., Yun, C.B., Roh, Y. and Lee, J.J. (2005), “Health monitoring of steel structures using impedance of thickness modes at PZT patches”, *Smart Struct. Syst*., **1**(4), 339-353.

Patel, H.H., Bland, C.H. and Poole, A.B. (1995), “The microstructure of concrete cured at elevated temperatures”, *Cement Concrete Res*., **25**(3), 485-490.

Piezo System (2009), *Product catalog*, http://www.piezo.com.

Rickli, J.L. and Camelio, J.A. (2009), “Damage detection in assembly fixtures using non-destructive electromechanical impedance sensors and multivariate statistics”, *Int. J. Adv. Manuf. Tech*., **42**(9-10), 1005-1015.

Rossi, P. (1991), “Influence of cracking in the presence of free water on the mechanical behaviour of concrete”, *Mag. Concrete Res*., **43**(154), 53-57.

Safiuddin, M. and Hearn, N. (2005), “Comparison of ASTM saturation techniques for measuring the permeable porosity of concrete”, *Cement Concrete Res*., **35**(5), 1008-1013.

Shin, S.W., Qureshi, A.R., Lee, J.Y. and Yun, C.B. (2008), “Piezoelectric sensor based nondestructive active monitoring of strength gain in concrete”, *Smart Mater. Struct*., **17**(5).

Simmers Jr., G.E. (2005), *Impedance-based structural health monitoring to detect corrosion*, Master’s Thesis, Center for Intelligent Material Systems and Structures, Virginia Polytechnic Institute and State University.

Soh, C.K. and Bhalla, S. (2005), “Calibration of piezo-impedance transducers for strength prediction and damage assessment of concrete”, *Smart Mater. Struct*., **14**(4), 671-684.

Sohn, H., Kim, S.D., In, C.W., Cronin, K.E. and Harries, K. (2008), “Debonding monitoring of CFRP strengthened RC beams using active sensing and infrared imaging”, *Smart Struct. Syst.*, **4**(4), 391-406.

Sun, F.P., Chaudhry, Z., Liang, C. and Rogers, C.A. (1995), “Truss structure integrity identification using PZT sensor-actuator”, *J. Intel. Mat. Syst. Str*., **6**(1), 134-139.

Tawie, R. and Lee, H.K. (2010), “Monitoring the strength development in concrete by EMI sensing technique”, *Constr. Build. Mater*., **24**(9), 1746-1753.

Tawie, R., Lee, H.K. and Park, S. (2009), "Using PZT sensors for detecting defects and characterizing quality of concrete", *Proceedings of the 5th International Workshop on Advanced Smart Materials and Smart Structures Technologies*, Boston, MA, USA, July.

Tseng, K.K.H. and Naidu, A.S.K. (2002), "Non-parametric damage detection and characterization using smart piezoceramic material", *Smart Mater. Struct*., **11**(3), 317-329.

Tseng, K.K., Basu, P.K. and Wang, L. (2002), "Damage identification of civil infrastructures using smart piezoceramic sensors", *Proceedings of the 1st European Workshop on Structural Health Monitoring*, France, July.

Yaman, I.O., Hearn, N. and Aktan, H.M. (2002), "Active and non-active porosity in concrete Part I: Experimental evidence", *Mater. Struct*., **35**(2), 102-109.

Yang, Y., Lim, Y.Y. and Soh, C.K. (2008), "Practical issues related to the application of the electromechanical impedance technique in the structural health monitoring of civil structures: I. Experiment", *Smart Mater. Struct*., **17**(3).

CC